MECHANICAL BEHAVIOR OF THE TI-6AL-4V TITANIUM ALLOY WITH MICROSTRUCTURAL EVOLUTION MODELING UNDER HOT AND SUPERPLASTIC CONDITIONS

Marcio Santos, marciowagner@usp.br[1]
Vincent Velay, vincent.velay@mines-albi.fr[2]
Gérard Bernhart, gerard.bernhart@irt-saintexupery.com[2]
Vanessa Vidal, vvidal@mines-albi.fr[2]
Hiroak Matsumoto, matsu_h@eng.kagawa-u.ac.jp[3]
Gilmar Batalha, gfbatalha@gmail.com[1]

[1]Polytechnic School of Engineering, University of Sao Paulo, Brazil
[2]Institut Clément Ader -Albi, France Inss for third author
[3]Kagawa University, Kagawa Department of Advanced Materials Science, Japan

Abstract. *The present work aims at evaluating and understanding the mechanical behavior of Ti-6Al-4V alloy under hot and superplastic forming conditions. Tensile tests were thus performed at temperature range from 650°C to 950°C at strain rates between 10^{-2} s^{-1} and 10^{-4} s^{-1}. Three equiaxed microstructures each characterized by a different starting grain size (4.88 µm, 3.0 µm and 0.5 µm) are compared and allow to obtain an understanding on microstructure evolution under hot and superplastic forming conditions. An accurate material model with microstructural considerations is proposed. The model capabilities consider the grain size evolution that is influenced by the temperature and the deformation. The computed flow stresses strongly depend on the strain rate but also on the considered initial grain size. Temperature and strain rate conditions may lead to a strain hardening phenomenon in some cases. The comparison between the model response and experiment shows a good agreement for all the tests carried out on the Ti-6Al-4V.*

Keywords: *Titanium, mechanical behaviour, microstructure, microstructural evolution, Ti-6Al-4V*

1. INTRODUCTION

During the hot forming the temperature of plastic forming depends on the particular alloy and its type, formability and required properties. Ti–6Al–4V alloy is usually Ti–6Al–4V alloy is a typical α + β titanium alloy, wherein element Al acts as a stabilizer and element V acts as b stabilizer (Alabort, Putman, and Reed 2015) (see Fig. 1). Attractive properties such as high strength to weight ratio, good fatigue properties and excellent corrosion resistance have made Ti–6Al–4V a leader in the manufacturing of aerospace components. Development of plastic forming technology contributes significantly to manufacturing titanium alloy products of high performance with low cost and short cycle. In plastic forming process of Ti alloys, the temperature control is essential due to undergoing phase transformations that may cause degradation of mechanical properties or even embrittlement formed in the temperature range of 940–980 °C (Nicolas 2010).

In the present work, a series of tensile test of Ti–6Al–4V alloy with a high temperature and lower strain rate were performed in a MTS machine to analyze the thermo-mechanical behavior under hot forming conditions on 700 °C to 950 °C and strain rate 10-2 s-1 to 10-4 s-1. In addition, the microstructural model was programmed into finite element codes, and then a series of simulations for grain growth evolution in the tensile test under different deformation conditions were performed. The theoretical predictions and simulation results of microstructural evolution were shown to be in agreement with experimental observations (see Fig. 2).

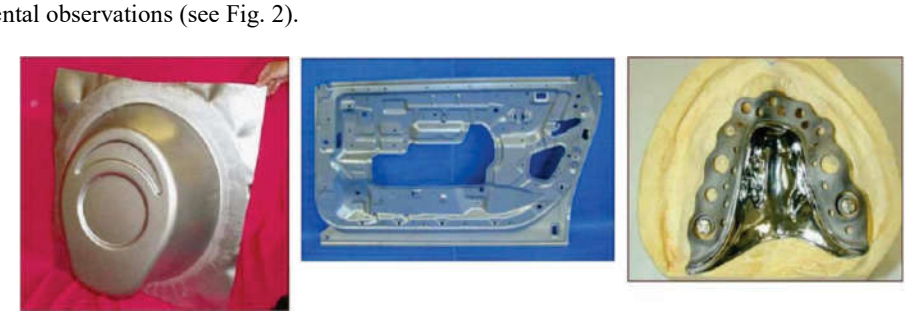

Fig. 1 : The different component of the superplastics titanium alloys (adapted from (Bonet et al. 2006))

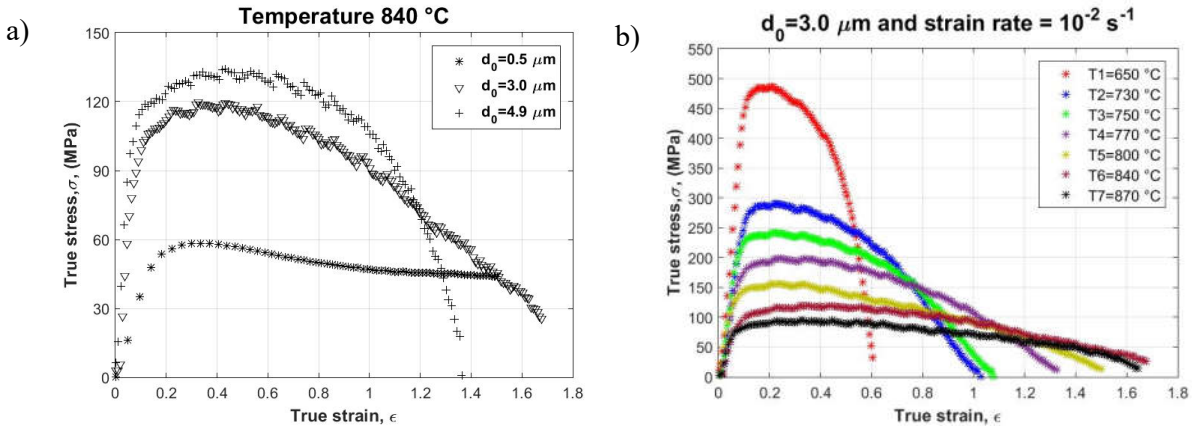

Fig.2 a) Influence of the starting microstructure and b) Influence of the test temperature

It considers three different equiaxed starting microstructure with initial average α grain sizes 0.5; 3.0 and 4.8 µm. For quantified the grain growth of Ti–6Al–4V alloy using high (SEM) magnifications, and summarized the relationships between microstructural evolution and strain rates and temperatures. The grain boundary sliding and grain growth play an important role on the occurring flow stress and hardening (Lin, Zhu, and Zhan 2011). From these observations, a program code Zmat developed in the Institut Clement Ader were used for identified the influence of the starting microstructure and its evolution on the mechanical of Ti-6Al-4V alloy. The grain growth effect is take into account through the evolution laws of the literature (S.L. Semiatin et al. 2010)(S. Lee Semiatin and Sargent 2010)(Bruschi et al. 2014).

A typical chemical composition for Ti-6Al-4V titanium alloy investigated in the present work is referred to table1. Three different equiaxed α grain starting microstructures are compared.

The microstructure is identified by Scanning Electron Microscopy (SEM) observations on mode secondary electron. It allows the comparison with starting microstructure and also its evolution microstructural.

2. MATERIALS AND PROCEDURE

The mechanical tensile tests were performed using a servo-hydraulic testing machine and a furnace accurate for the very large elongations. It includes three heating zones controlled by S- thermocouples and allows to maintain a constant temperature during all the sample deformation. As the use of a classical extensometer was not possible due to the very large elongation, a nonlinear crosshead displacement was considered for all the mechanical tests in order to obtain a constant target strain rate $\dot{\varepsilon}$ at the center of the specimen. Thus, the time variation of applied displacement u(t) was provided by Eq.1 . Afterwards, the true strain ε_t and the true stress σ_t evolutions were calculed from the value of displacement *u(t)* given by the previous equation (Eq. 2 and Eq. 3).

$$u(t) = l_0\left(e^{\dot{\varepsilon}t} - 1\right) \quad (1)$$

Where

- l_0 is the initial gauge length
- $\dot{\varepsilon}$ is the target strain
- t is the time

$$\varepsilon_t = log\left(1 + \frac{u(t)}{l_0}\right) \quad (2)$$

$$\sigma_t = \frac{F}{S_0}\left(1 + \frac{u(t)}{l_0}\right) \quad (3)$$

Where F is the strength registered by the load sensor of the equipment and S0 the initial section of the specimen.

Materials and testing. A plate with a thickness of 4 mm was hot-rolled to provide the Ti-6Al-4V alloy sheets. Three different microstructures were compared, the first one, hereafter designed as kind of micro structure, hereafter designed as UltraFine-Grained Microstructure (UFGM) (Fig. 3a), was obtained using a combined Forging-rolling process providing plates with a thickness from 1.4 mm to 1 mm and an average grain size 0.5 µm from (Matsumoto, Velay, and Chiba 2014). A second and third (Fig. 3 b and 3c) Starting Microstructure (SM), was the most widely used under Superplastic Forming conditions. It considers equiaxed (α+β) Ti-6Al-4V alloy with an average a-phase grain size of 3 µm and 4.9 µm, respectively (Santos et al. 2015)(Velay et al. 2016).

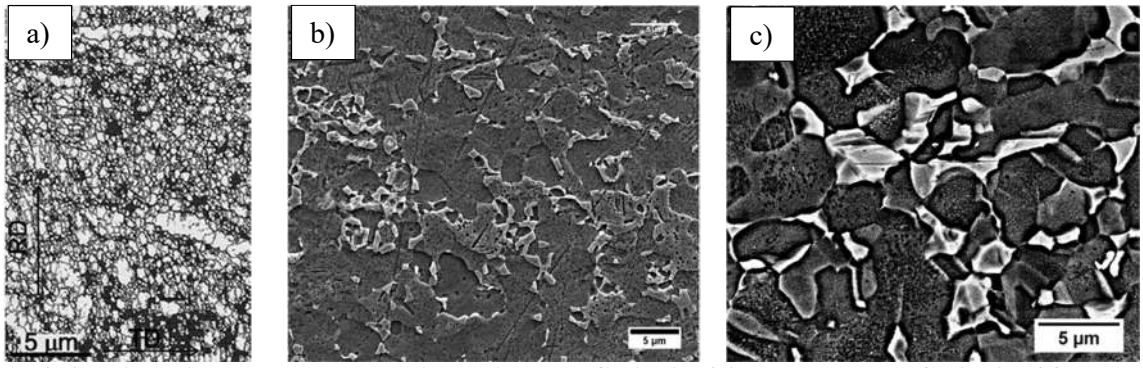

Fig. 3: Starting Micro structure: UltraFine grained (a); Grain size 3.0 µm and (b) and Grain size 4.8 µm (c)

All the test conditions are illustrated in table 1. The levels of temperatures from 700°C to 950°C and different strain rates from 10^{-4} s^{-1} to 10^{-2} s^{-1} were considered. The comparison between three microstructures (0.5 µm and 3.0; 4.9 µm) was only performed at the higher test temperature about 870°C.

Table 1 - Dynamic test conditions, for an initial grain size of d0= (# 0.5 ; × 3.0 ; * 4.9 µm)

	T (°C)							
Strain rate	700	770	800	840	850	870	920	950 vacuum
$\dot{\varepsilon} = 10^{-2}\ s^{-1}$	*#	×	×*	×*#	×	×*	×	
$\dot{\varepsilon} = 5.10^{-3}\ s^{-1}$	#							
$\dot{\varepsilon} = 10^{-3}\ s^{-1}$	*#	×	×*	×*#	×	×*	×	*
$\dot{\varepsilon} = 5.10^{-4}\ s^{-1}$	#							
$\dot{\varepsilon} = 10^{-4}\ s^{-4}$	*#	×	×*	×*#	×*#	×*	×	*

Depending on the microstructure, some of the mechanical tests were performed at the Clément Ader Institute, other ones were conducted at the Tohoku University. The capabilities of each equipment are similar, the main difference concerns the sample shape.

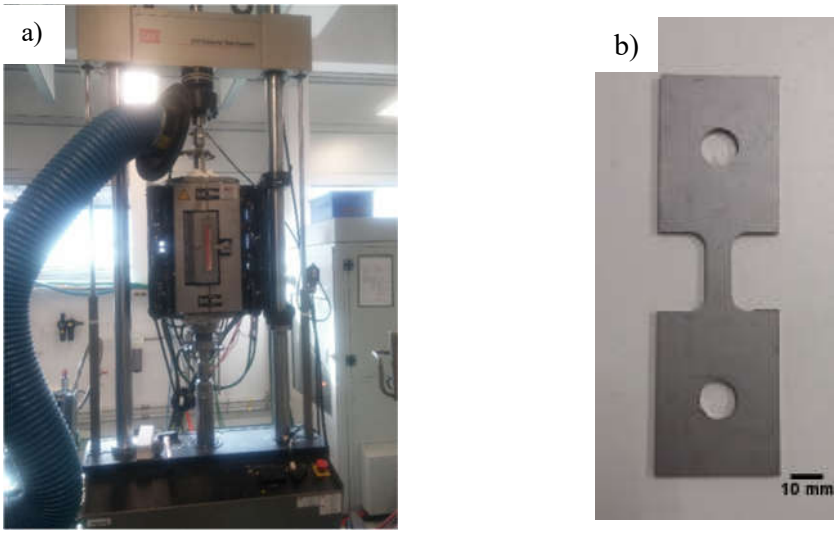

Fig. 4: Experimental Set-up (a); Sample used for the mechanical tests at the Clément Ader institute (b)

Thus, grain growth is investigated by conducting static and dynamic tests. The static tests consider the different temperature exposure time regarding the forming time during the process. The grain growth evolution for the static tests at T = 870 °C and the several temperature exposure times t = 120 s (a), t = 2,100 s (b), t = 23,4000 s (c) (see Fig. 5).

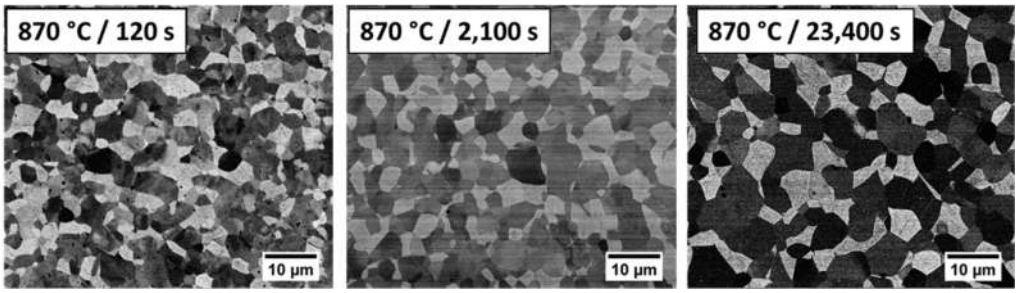

Fig. 5 - Static tests: grain Coarsening evolution.

The grain growth evolution for the case of the dynamic tests at T = 870 °C and several strain rates (= 10−2 s−1 (a), = 10−3 s−1 (b) and = 10−4 s-1 (c)) (see Fig. 6)

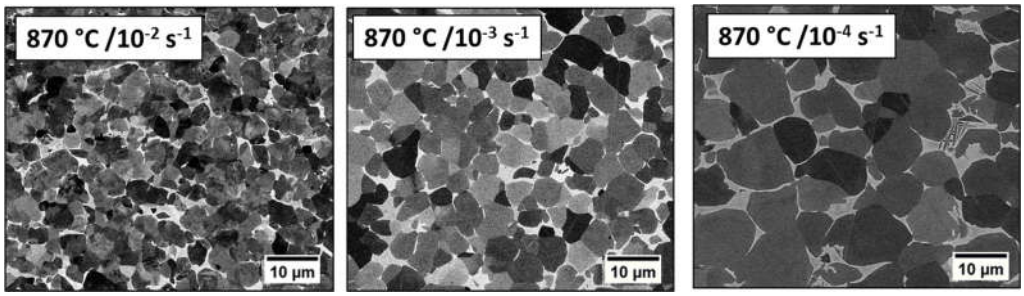

Fig. 6 - Dynamic test coarsening evolution grain

3. GRAIN GROWTH PREDICTIONS UNDER DYNAMIC CONDITION

The grain growth is defined as an internal variable of the behavior model. In this section, the grain growth evolution model based on Semiatin's (S. Lee Semiatin and Sargent 2010) (Chen, Chen, and Lin 2010) empirical law (see Fig. 7) is used to compute the coefficient identification for the grain growth evolution law. Moreover, the results are compared with the observations performed.

$$d^3(t) - d_0^3 = K_s(T).t \quad (4)$$

$$\dot{d}_s = A_1 d^{-m_1} \quad (5)$$

Where A_1 and m_1 depend on temperature (T)

Tab. 2 Extrapolation values for the initial grain size and K_s

d_0 (µm)	2.5	2.5	3.0
K_s (T °C)	K_s (775)	K_s (815)	K_s (920)

Comparison of computed grain growth-time (Fig. 8) and computed grain growth-strain curves using the evolution law identified with the coarsening rate constants by (Semiatin et al) and the experimental measurements performed from 700 to 920 °C and d_0 = 3µm.

4. Microstructural evolution under dynamic (d_d) conditions

Table 3 and Fig. 9 show the extrapolation of the initial grain size values for the dynamic coarsening coefficient (K_d).

$$d^3(t) - d_0^3 = K_d(T).t \quad (6)$$

$$\dot{d}_d = A_2 d^{-m_2} \dot{p}^{n_1} \quad (7)$$

Tab. 3 Extrapolation values for the initial grain size and K_d

d_0 (µm)	2.5	2.5	3.0
K_d(T °C)	K_d (775)	K_d (815)	K_d (920)

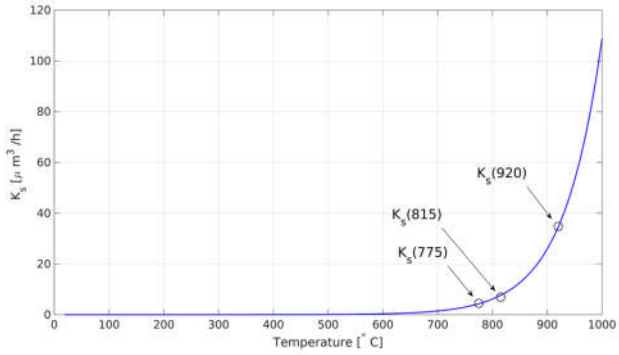

Fig. 7 Grain growth prediction under static conditions

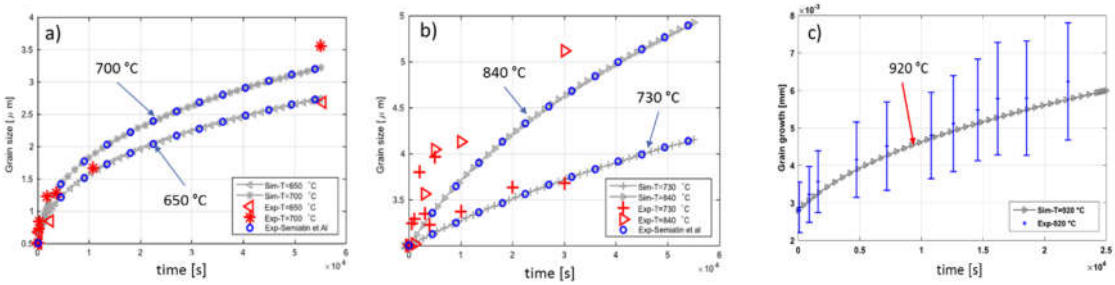

Fig.8 Comparisons between model prediction and experimental measurements

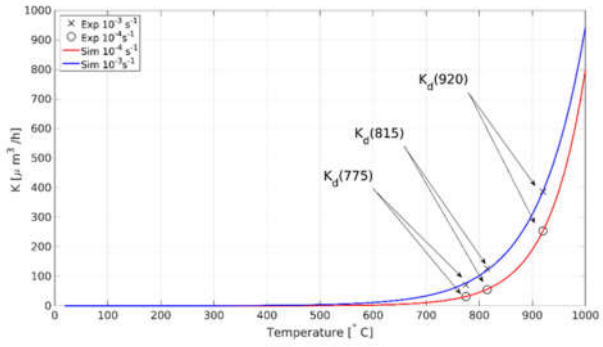

Fig. 9 - Grain growth prediction under dynamic conditions

The comparison of the computed grain growth-time (see Figures 10a and 10c) and the computed grain growth-strain (Figures 10b and 10d) curves, using the evolution law identified with the coarsening rate constants by (Semiatin et al) and the experimental measurements performed at 920 °C and do = 3µm (Figures10a and 10b); at 800 °C and d_o = 4.9 µm (Figures 10c and 10d).

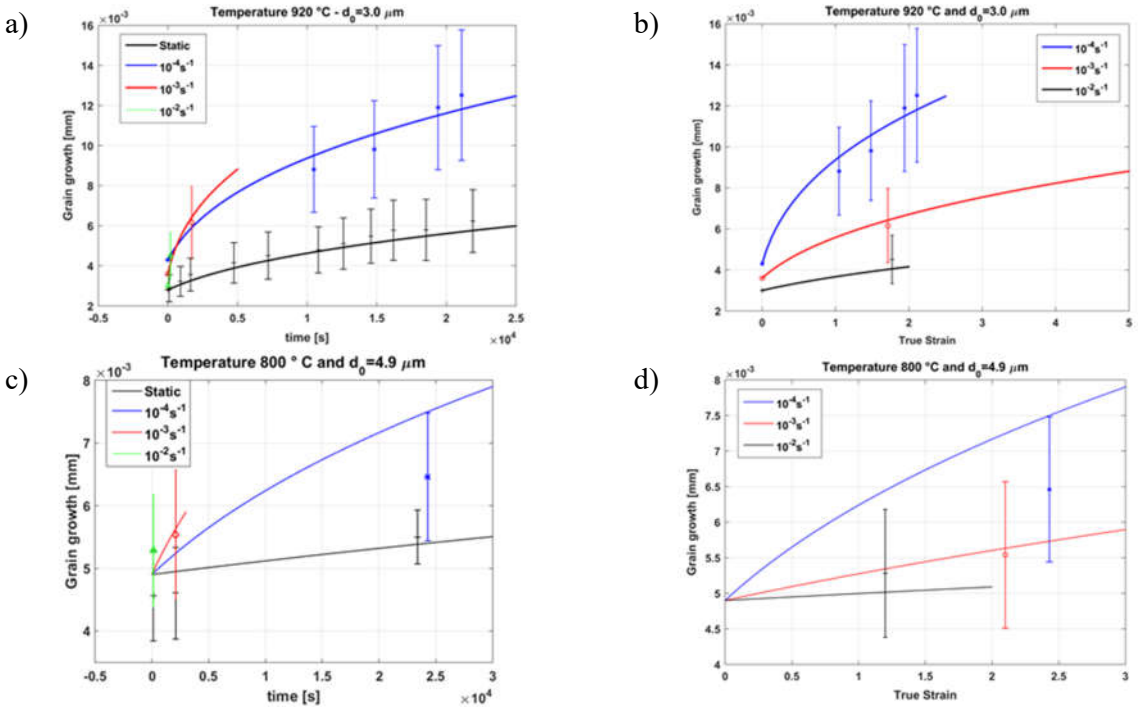

Fig. 10 - The dynamic grain growth (Eq. 7) allows reproducing grain growth kinetics over a range of temperatures and strain rates.

5. RESULTS

The stress-strain response for 4.9 and 3.0 µm grain size microstructures and temperatures from 800 to 870°C. For this, the strain rate sensitivity of the materials was quite significant (see Fig 11).

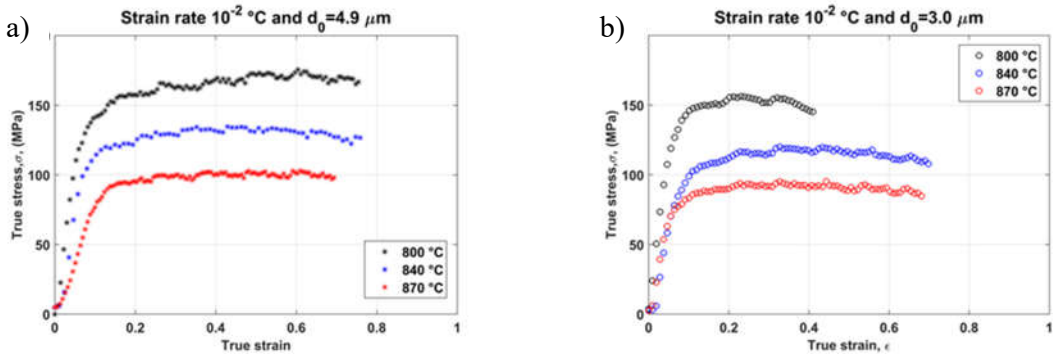

Fig. 11 - Comparison between the computed true strain - true stress curves for two starting grain sizes: 4.9 (a) and 3.0 µm (b) testes at the temperatures: 800, 840 and 870 °C.

Fig 12 shows that UFGM allows a very important elongation whatever the strain rate considered. Indeed, even for the higher strain rate, an elongation of around 60% can be reached, whereas necking occurs from an elongation of 20% for the initial microstructure under the same test conditions. Moreover, UFGM exhibits a second hardening phase occurring for the lower temperatures. This effect is mainly due to the increase of the grain size activated by the high temperature exposure time of $\dot{\varepsilon} = 5.10^{-4}$ s^{-1} and 10^{-4} s^{-1}.

Table 4 presents the Model approach for the unified superplastic constitutive equations.

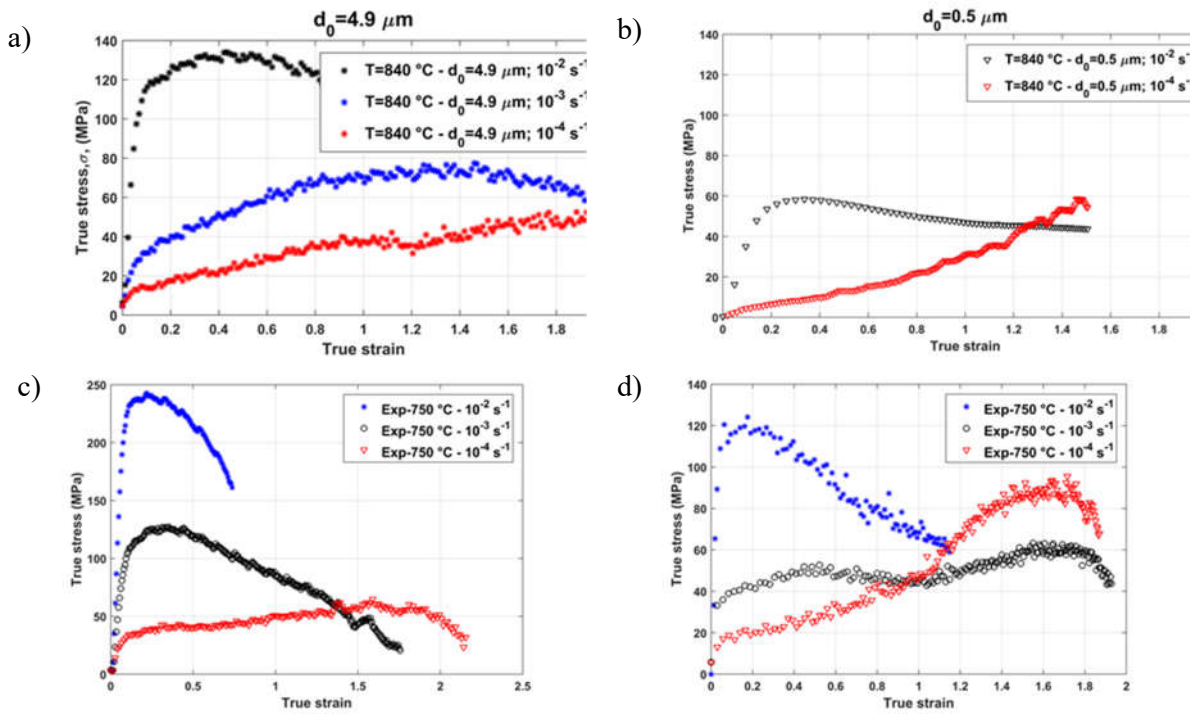

Fig. 12 - The effect of start grain size on stress-Strain response: 4.9 µm and 0.5 at 840 (a, b) and 3.0 µm and 0.5 µm at 750 (c,d) for different strain rates.

Table 4 - Model unified superplastic constitutive equations.		
Yield criterion	$\mathbf{f = \sigma_{eq} - R - \sigma_0} \Rightarrow$ $\boldsymbol{\sigma_{eq} = \sqrt{\frac{3}{2} S : S}}$	(8)
Isotropic Hardening variable:	$\boldsymbol{R = Q\left(1 - e^{-bp}\right)}$	(9)

Associated strain rule	$\mathbf{D_p} = \frac{3}{2}\dot{\mathbf{p}}\frac{\mathbf{S}}{\sigma_{eq}}$ and $\dot{p} = \langle\frac{f}{K}\rangle^{n}$	(10)
Corotational stress rate	$\overset{\nabla}{\boldsymbol{\sigma}} = 2GD_e + \lambda Tr(D_e)$	(11)
Strain rate partition	$D_e = D_t - D_p$	(12)
($\dot{d}_s$) Atomic diffusion grain boundary mobility ($\dot{d}_d$) grain growth kinetics A_i; m_i and n_i temperature parameter P – effective inelastic strain	$\dot{d} = \dot{d}_s + \dot{d}_d$ $\dot{d}_s = A_1 d^{-m_1}$ $\dot{d}_d = A_2 d^{-m_2}\dot{p}^{n_1}$	(13)
Influence on the viscous flow:	$\dot{p} = \langle\frac{f}{K}\rangle^{n}$; $K = K_r\left(\frac{d}{\chi(d_0)}\right)^{\frac{\mu}{n}}$; $n = n_r\left(\frac{d}{\chi(d_0)}\right)^{\alpha}$; $\chi(d_0) = \chi_1 e^{-\chi_0 d_0}$;	(14)
Influence on the hardening	$R = Q(1 - e^{-bp})$ => $Q = Q_0 e^{\gamma\Delta d}$ Where $\Delta d = d - d_0$	(15)

Fig. 13a does not show a deformation mechanism change for the initial grain size of d_0= 4.9µm, whereas in Fig. 13b, this effect is observed and well assessed at low strain rate (10^{-4} s^{-1}) for an initial grain size of d_0= 0.5µm.

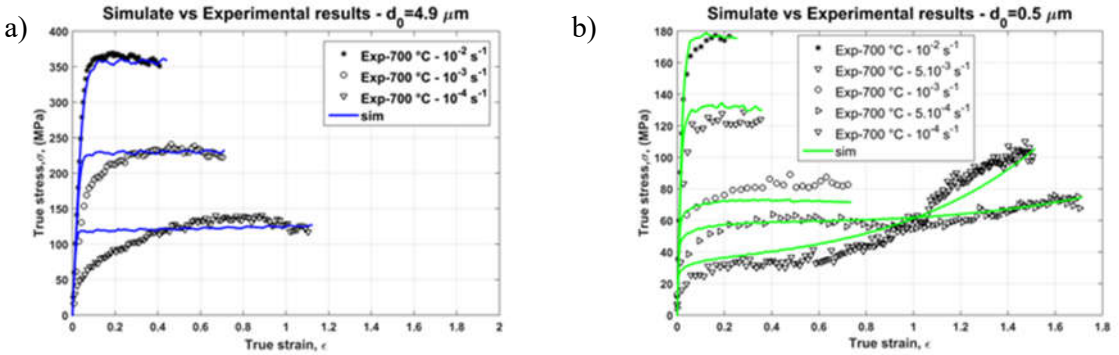

Fig. 13 Computed Strain-Stress data vs Experimental results at a temperature of 700 °C and initial grain size of d_0=0.5 (a) and 4.9 µm (b).

For the case of the 0.5 µm starting, the behavior model is observed to predict a stress decrease under certain conditions (see Fig 14a at 10^{-2} s^{-1}). This is due to the time-strain applied to the simulation, inducing a slight strain rate decrease with the sample elongation as mentioned previously.

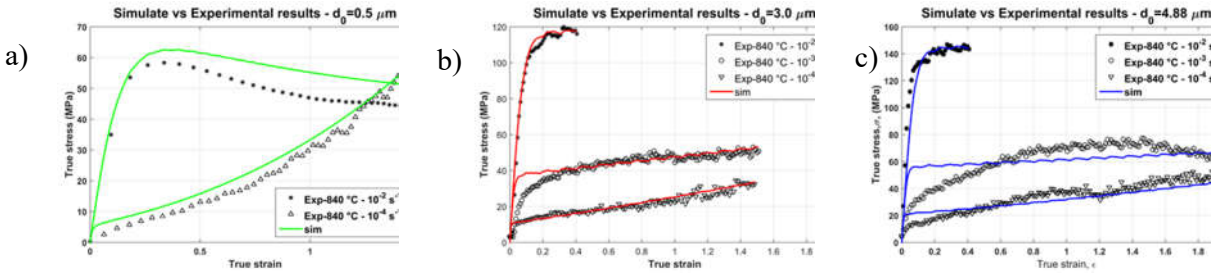

Fig. 14a Computed strain-stress datas vs Experimental results at a temperature of 840 °C and initial grain size of d_o=0.5 µm

Fig. 14b Computed Strain-Stress datas vs Experimental results at a temperature of 840 °C and initial grain size of d_o =3.0 µm

Fig. 14c Computed strain-stress datas vs Experimental results at a temperature of 840 °C and initial grain size of d_o =4.9 µm

6. CONCLUSOIONS

The superplastic behavior of a Ti–6Al–4V Titanium alloy was investigated under hot forming conditions regarding three different starting microstructures with an average α grain size of 0.5; 3 and 4.9 µm. A temperature range of 700 to 950 °C and strain rates between 10^{-4} to and 10^{-2} s^{-1} were considered.

The parameters of a grain growth model are identified the measurement performed successfully describes the evolutions predicted by Semiatin et al (S. Lee Semiatin and Sargent 2010).

The internal variable related to grain growth was introduced into the mechanical model through the viscous flow.

The stability of the constitutive equations is investigated under uniaxial conditions by the prediction of the necking and by analyzing the shrinkage rate against the normalized cross-sectional area.

- The strain-stress response exhibits a viscous flow dependent on the test temperature, the initial microstructure and the grain growth.
- A strain hardening is observed for the initial time period test due to the grain growth evolution.

For the Ti–6Al–4V superplastic forming (SPF) under a strain rate ($\dot{\varepsilon}$) ranging from 10^{-4} s^{-1} to 10^{-2} s^{-1}:

- The viscous flow was dependent on the initial microstructure and its evolution;
- The strain hardening was observed during the beginning of the test due to the grain growth evolution.

7. ACKNOWLEDGEMENTS

Marcio Santos acknowledges his ongoing scholarship and financial support from the Brazilian Federal Agency for Support And. Evaluation of Graduate Education - CAPES (Coordination for the Improvement of Higher Education Personnel).

8. REFERENCES

Alabort, E., D. Putman, and R.C. Reed. 2015. “Superplasticity in Ti-6Al-4V: Characterisation, Modelling and Applications.” *Acta Materialia* 95: 428–42.

Bonet, Javier et al. 2006. “Simulating Superplastic Forming.” *Computer Methods in Applied Mechanics and Engineering* 195(48–49): 6580–6603.

Bruschi, S. et al. 2014. “Testing and Modelling of Material Behaviour and Formability in Sheet Metal Forming.” *CIRP Annals - Manufacturing Technology* 63(2): 727–49.

Chen, DC C D.-C., WJ J Chen, and JY Y Lin. 2010. “Finite Element Analysis of Superplastic Blow-Forming of Ti-6Al-4V Sheet into Closed Ellip-Cylindrical Die.” *International Journal of ...* 9(1): 17–27. http://www.ijsimm.com/Full_Papers/Fulltext2010/text9-1_17-27.pdf (November 22, 2012).

Lin, J., T. Zhu, and L. Zhan. 2011. Superplastic Forming of Advanced Metallic Materials *Superplastic Forming of Advanced Metallic Materials*. Elsevier. http://www.sciencedirect.com/science/article/pii/B978184569753250008X (January 30, 2015).

Matsumoto, Hiroaki, Vincent Velay, and Akihiko Chiba. 2014. “With an Ultrafine-Grained a -Single Phase Microstructure during Low-Temperature-High-Strain-Rate Superplasticity.” *JOURNAL OF MATERIALS&DESIGN* 66: 611–17.

Nicolas, Clément. 2010. “Phase Transformations and Mechanical Properties of the Ti-5553 β-Metastable Titanium Alloy.” University Catholique de Louvain.

Santos, Marcio et al. 2015. “THE INFLUENCE OF LOW STRAIN RATE AND HIGH TEMPERATURE ON MICROSTRUCTURAL EVOLUTION OF TI--6Al--4V TITANIUM ALLOY.” In *Advances in Materials and Processing Technologies*, ed. IMDEA Materials Institute and Universidad Carlos. Madrid, 103.

Semiatin, S. Lee, and Gordon a. Sargent. 2010. “Constitutive Modeling of Low-Temperature Superplastic Flow of Ultrafine Ti-6Al-4V Sheet Material.” *Key Engineering Materials* 433: 235–40.

Semiatin, S.L. et al. 2010. “Plastic Flow and Microstructure Evolution during Low-Temperature Superplasticity of

Ultrafine Ti-6Al-4V Sheet Material." *Metallurgical and Materials Transactions A* 41(2): 499–512.
Velay, V., H. Matsumoto, V. Vidal, and A. Chiba. 2016. "Behavior Modeling and Microstructural Evolutions of Ti--6Al--4V Alloy under Hot Forming Conditions." *International Journal of Mechanical Sciences* 108–109: 1–13.

9. RESPONSIBILITY NOTICE

The authors are the only responsible for the printed material included in this paper.